

# Chain Orientation and Its Effect on Mobility at a Rubbed Surface

Y. Pu, H. White, M. H. Rafailovich,\* and J. Sokolov\*

Department of Materials Science and Engineering, State University of New York, Stony Brook, New York 11794-2275

S. A. Schwarz

Department of Physics, Queens College of CUNY, Flushing, New York 11367

A. Dhinojwala

Department of Polymer Science, University of Akron, Akron, Ohio 44325-3909

D. M. G. Agra and S. Kumar

Kent State University, Kent, Ohio 44242

Received November 29, 2000; Revised Manuscript Received March 5, 2001

**ABSTRACT:** We have measured the tracer diffusion coefficient in PS films oriented by surface rubbing. The results show that the diffusion perpendicular to the rubbed surface is slower in oriented than in nonoriented chains. The decrease of the diffusion coefficient was correlated with the total oriented volume as determined by birefringence measurements.

## Introduction

Polymer thin films are important in numerous commercial applications relating to coating, adhesion, and lubrication. As the films are becoming increasingly thinner, several authors<sup>1–6</sup> have shown that configuration effects can begin to dominate the dynamics. There is general agreement that the dynamics of polymer chains are greatly reduced when the chains are absorbed at an attractive interface.<sup>1,3</sup> There is much more controversy on the nature of the dynamics at the free surface.<sup>2,4–8</sup> In interpreting the results, it is important to discriminate between properties that involve short-range relaxation, such as the glass transition,  $T_g$ , or the dielectric constant, and those where long-range motion of the polymer is involved, such as center-of-mass diffusion or the expansion coefficient. For example, it is obvious that, for a grafted polymer brush, the segmental mobility will undergo a change around  $T_g$  with increasing temperature while the center-of-mass mobility or the expansion coefficient is severely limited. Similarly, when polymer chains are oriented by rubbing, reorientation involves motion on both short and long length scales. Local fluctuations, such as the reorientation of the  $\pi$  system about the chain axis,<sup>7–10</sup> are involved in the motion on the scale of the monomer. Longer range orientation, such as entire chain axis alignment,<sup>10–12</sup> is on the scale of the polymer chain. Finally, the motion of center-of-mass of the polymer chain is on the scale of the diffusion distance.

The relaxation process of polystyrene (PS) segments at a rubbed surface was investigated using near-edge X-ray absorption fine structure (NEXAFS) spectroscopy.<sup>7</sup> Dhinojwala et al.<sup>8</sup> discussed the relaxation dynamics in rubbed thin films with optical birefringence measurements. NEXAFS is sensitive to local motion of the polymer; the optical birefringence results are sensitive mostly to the reorientation of the phenyl rings perpendicular to the C–C bonds of the repeat unit as well. It is much more difficult to extract information on

center-of-mass mobility of the chains in a direction perpendicular to the orientation. In this paper, we address this topic using dynamic secondary ion mass spectrometry (DSIMS). We directly measured the tracer diffusion on rubbing-modified surfaces in a direction perpendicular to the plane of the induced orientation. The degree of orientation was measured by optical birefringence and correlated to the tracer diffusion coefficients. The results were then compared with the surface relaxation process as observed through atomic force microscopy (AFM) and shear modulation force microscopy (SMFM).

## Sample Preparation and Experimental Setup

Multilayer samples, shown in the inset of Figure 1, were prepared as follows: a layer of hydrogenated polystyrene (hPS,  $M_w = 168K$ , thickness = 200 nm) was spun-cast directly onto a 2 in. square glass slide. Glass is chosen since the substrate has to be optically clear for the birefringence measurements. The thickness of the hPS, 200 nm, was chosen to eliminate the effect of the rubbing on the middle layer, which is not expected to propagate more than 60 nm into the film.<sup>11</sup> A film composed of a blend of 80% hPS, with the same molecular weight as the matrix, and 20% deuterated polystyrene (dPS,  $M_w = 94K$ , thickness = 28 nm) was spun-cast onto another glass slide and scored. Half the film was floated onto the first hPS layer, which was preannealed at 423 K for 30 min to prevent the separation of the layer from the glass substrate, while the subsequent layers were floated. Another hPS film with the same thickness and  $M_w$  as the first layer was floated on top of the dPS from distilled water. The second half of the dPS film was then floated on top of the hPS layer. In this method, we could simultaneously measure the diffusion coefficient of the rubbed chains near the PS–vacuum interface and the PS chains in the bulk which are not affected by the rubbing process.

The samples were rubbed using a metal cylinder wrapped in velvet cloth with an applied normal force. The cylinder was spun at a constant angular velocity of 550 rev/min, while moving across the sample surface at a constant velocity,  $v = 0.9$  m/min, in the rubbing direction. To get films with different deformation, the number of rubbing cycles with the same pressure was varied.

A photoelastic modulator (PEM 90, Hinds Instruments) with a fused silica head and a He-Ne laser (wavelength  $\lambda = 632.8$  nm) was used for the optical phase retardation measurements. The photoelastic modulator (PEM) was placed between two crossed polarizers with its optical axis at  $45^\circ$  to the axes of polarizer and analyzer. The sample cell with the rubbed multilayer sample was placed between the PEM and the analyzer. The signal from the photodetector was fed into a lock-in amplifier (EG&G Princeton Applied Research, model 5210) for measurement of the ac signal and into a digital multimeter for the dc signal. The lock-in amplifier was tuned to the 50 kHz reference signal from the PEM. The laser beam was incident normal to the sample cell's surface. The signal was monitored while rotating the sample with respect to the surface normal. The sensitivity of this method enables us to measure the phase retardation with a precision of  $\pm 0.01^\circ$ .

Tracer diffusion was then allowed to occur by annealing the samples in a vacuum of  $10^{-6}$  Torr at 407 K for several hours. The concentration profiles of the dPS were measured using DSIMS (Atomika 3000-30 ion microprobe) with a 2 keV, 20 nA,  $\text{Ar}^+$  beam at  $30^\circ$  off-normal incidence. The depth resolution was 8 nm at a sputtering rate of approximately 40 nm/h. The beam was rastered over a 1.0 mm square region with ions accepted from a 0.3 mm square region in the center of the sputtering crater. Negative secondary ions  $\text{H}^-$ ,  $\text{D}^-$ ,  $\text{C}^-$ ,  $\text{O}^-$ ,  $\text{Si}^-$ ,  $\text{CH}^-$ , and  $\text{CD}^-$  were detected with a quadrupole mass analyzer. A thin ( $\sim 35$  nm) sacrificial polystyrene layer is floated onto the polymer surface from deionized water, so that a steady-state sputtering condition can be attained prior to reaching the real film surface. In addition, the sacrificial layer also minimized artifacts induced by surface scratches produced while rubbing. The sample surface was flooded by an e-beam to reduce charging in the insulated glass substrate.

Shear modulation force microscopy (SMFM)<sup>13</sup> was performed to measure the surface creep as a function of temperature by laterally modulating the SFM cantilever and recording the modulation response as a function of temperature. The samples are placed on a heating stage (MMR Technologies model R2700-2) with temperature stability of 0.05 K. The SMFM head and the heating stage were located in a sealed glovebox, which was purged with dry nitrogen to reduce capillary condensation ( $<11\%$  relative humidity).

## Results and Discussion

**Birefringence Measurements on the Rubbed Surface.** It is well established that the rubbing process produces alignment in polymers by orientation of both the chain axis and molecular side groups, such as benzyl rings, on the polymer chains.<sup>7-10</sup> This induces birefringence as a consequence of the difference in refractive index for light polarized parallel and perpendicular to the orientation direction.<sup>11</sup> The induced birefringence can be quantified by measuring the optical retardation value,  $\delta$ , which detects the degree and direction of the orientation. It can be expressed as follows:

$$\delta = \int_0^{h/2} \frac{h/2}{\lambda} \Delta n(z) dz \quad (1)$$

where  $\Delta n(z)$  is the birefringence at a distance  $z$  from the surface,  $h$  is the overall film thickness, and the wavelength of the light used for this study was  $\lambda = 632.8$  nm. Van Aerle et al.<sup>11</sup> have shown that  $\Delta n$  saturates almost immediately in the top of the polymer, directly contacting the rubbing cloth. Additional rubbing will increase the extent of the oriented layer to a maximum depth which depends on the specific polymer used, while there is no detectable increase in degree of orientation within the top layers.  $\Delta n(z)$  can then be approximated as a constant over a distance  $Z_0$ , where  $Z_0$  increases with the number of rubbing cycles. Therefore,  $\delta$  can be a

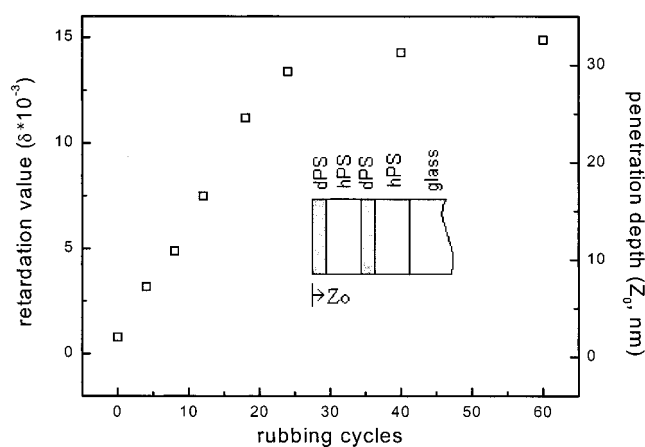


**Figure 1.** Optical phase retardation values and the estimated penetration depth<sup>8</sup> plotted as a function of the number of rubbing cycles.

measurement of the penetration depth of the alignment induced at the surface.

Figure 1 shows the absolute optical phase retardation value ( $\delta$ ) of the four-layer samples described previously as a function of the number of rubbing cycles that each sample had experienced. The actual measured value of  $\delta$  is negative, which is consistent with the sign of the retardation for oriented PS chains. As discussed previously,<sup>8,11,14</sup> this rules out the positive "form birefringence" associated with surface roughness induced by rubbing. Hence, the birefringence observed is mostly due to the orientation of the PS chains. From the figure we can see that, as previously reported for a wide selection of polymer systems,  $\delta$  increases linearly with the number of rubbing cycles and then reaches saturation as the maximum penetration depth is reached. The lower limit of the maximum penetration depths, 32 nm, of the rubbed polystyrene film was calculated by Dhi-nojwala's group<sup>8</sup> by assuming that the polymer molecules in the 5.8 nm film is uniformly aligned throughout the whole film after rubbing. The actual penetration depth can be larger. We use this value to generate the depth scaling,  $Z_0$ , in Figure 1.

**Rubbing Effect on Diffusion Normal to the Surface.** Since the rubbed samples are consisted of alternating layers of dPS and hPS (see inset of Figure 1), we could now measure the diffusion coefficients simultaneously for labeled chains at two different distances from the sample surface. The result for a rubbed sample is shown in Figure 2. In the inset, we show the concentration profiles for a rubbed and non-rubbed sample near the vacuum interface. The solid triangle corresponds to a nonrubbed sample, and the open square corresponds to a sample rubbed for 60 cycles and having an optical retardation value of  $\delta = 0.015$ . Both the rubbed and nonrubbed samples were annealed at 407 K in a vacuum of  $10^{-6}$  Torr. From the figure, we can see that the middle layer is more diffused than the surface layer for the rubbed sample. The middle layer of dPS has broadened to the same extent in both rubbed and nonrubbed samples (not shown). The continuous lines in Figure 2 are fits to the solution of a Fickian equation for a thin film diffusing into an infinite/semiinfinite medium given by

$$\phi(x) = \frac{1}{2} \left[ \operatorname{erf} \left( \frac{h-x}{\sqrt{4Dt}} \right) + \operatorname{erf} \left( \frac{h+x}{\sqrt{4Dt}} \right) \right] \quad (2)$$

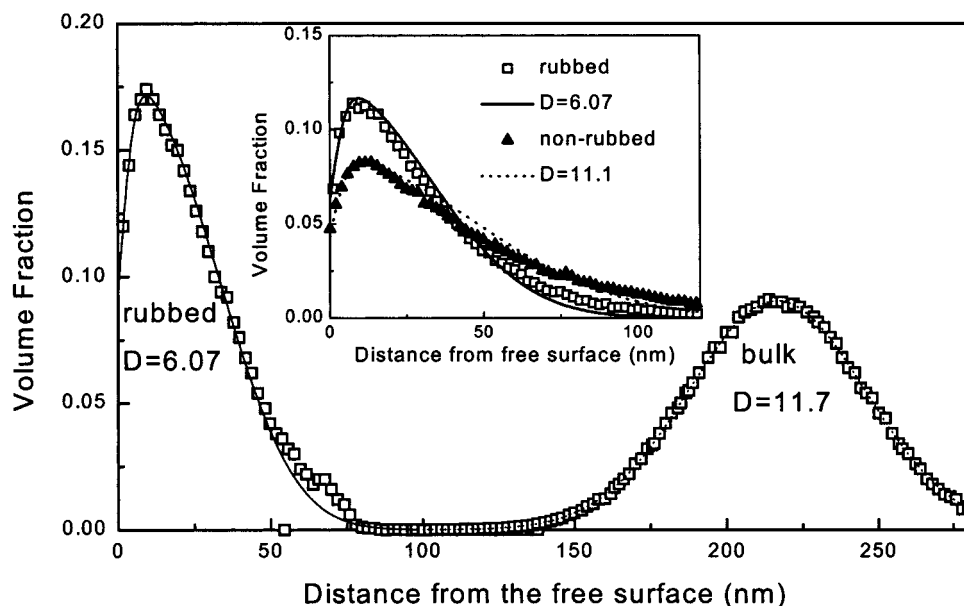


**Figure 2.** DSIMS concentration profiles of the dPS volume fraction as a function of distance from the surface for a rubbed four-layer sample. Inset: concentration profiles near the vacuum interface for the rubbed sample with  $\delta = 0.015$  ( $\square$ ) and the nonrubbed sample ( $\blacktriangle$ ). Both samples were annealed at 407 K. The unit of the diffusion coefficient is  $10^{-16} \text{ cm}^2/\text{s}$ .

where  $x$  is the distance away from the interface,  $D$  is the tracer diffusion coefficient, and  $h$  is the initial thickness of the tracer film for the top layer and half of the thickness for the middle layer. We obtain  $D_{\text{bulk}} = 11.7 \times 10^{-16} \text{ cm}^2/\text{s}$  for the middle layer, which is in agreement with reported bulk diffusion coefficient data at this temperature.<sup>15</sup> Examination of the depth profile near the vacuum interface indicates that less diffusion has occurred in rubbed than in the nonrubbed samples. Fits to eq 2 yields  $D_{\text{surf}} = 11.1 \times 10^{-16} \text{ cm}^2/\text{s}$ , which is very close to the value of the middle layer for the nonrubbed sample. For the rubbed surface, we get  $D_{\text{surf}} = 6.07 \times 10^{-16} \text{ cm}^2/\text{s}$ , which is approximately half of the bulk value. From Figure 1, we see that the value of  $\delta$  for this sample corresponds to an initial oriented thickness of 32 nm. This is comparable to the thickness of the entire dPS tracer layer. Clearly, the middle layer is far outside the region affected by the rubbing, and hence it is not surprising that  $D$  is bulklike.

In Figure 3a, we plot  $D_{\text{bulk}}/D_{\text{surf}}$ , the ratio of the diffusion coefficients obtained from the surface dPS layer and that from the "bulk" dPS layer in the same sample, as a function of the optical retardation value for samples subjected to different numbers of rubbing cycles. Each data point in Figure 3 represents the mean value of  $D_{\text{bulk}}/D_{\text{surf}}$  for three different samples having the same retardation values. From the figure, we see that for  $\delta < 0.0134$   $D_{\text{bulk}}/D_{\text{surf}}$  increases linearly and then reaches a saturation value for  $\delta > 0.0134$ , which is close to the maximum optical retardation saturation value shown in Figure 1.

On the basis of what is known from previous results regarding the rubbing mechanism,<sup>9,10</sup> we can propose a model to explain the rubbing effect on diffusion. There is general agreement that the polymer chain axis lies in the surface plane after the rubbing process. The results in Figures 2 and 3 clearly show that the tracer diffusion coefficient for center-of-mass motion in the direction perpendicular to the orientation plane is reduced relative to the value for nonoriented chains. Van Aerle et al.<sup>11</sup> have shown that the maximum orientation is achieved almost immediately in the top

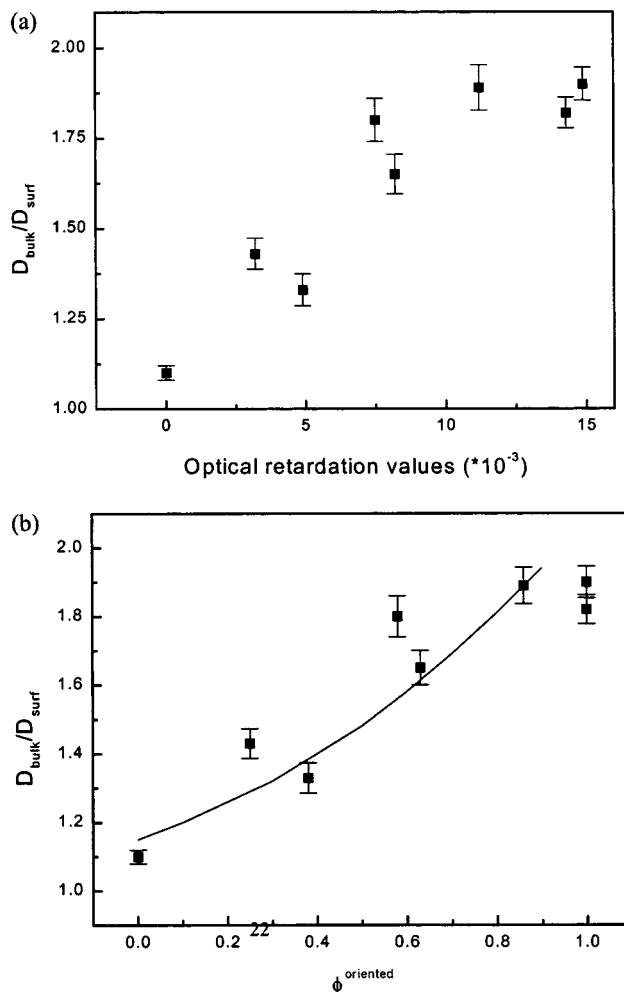


**Figure 3.** Ratio of the tracer diffusion coefficient in the center and at the surface of the sample,  $D_{\text{bulk}}/D_{\text{surf}}$ , as a function of (a) optical retardation value,  $\delta$ , and (b) oriented volume,  $\phi_{\text{oriented}}$ , as defined in the text. The solid line in (b) is the fit to eq 3.

layer. Additional rubbing simply increases the volume of oriented chains, but not the degree of orientation.



Likewise, the dependence of  $D_{\text{bulk}}/D_{\text{surf}}$  on  $\delta$  plotted in Figure 3a can be interpreted in terms of an increase in the volume of oriented chains rather than the degree of orientation of individual chains involved in the diffusion. Implicit in this assumption is that all chains in the volume affected by rubbing are oriented to the same degree. We can therefore divide the data into two regimes. When  $\delta > 0.0134$ , the oriented thickness, 32 nm, is comparable to or slightly larger than  $L_0 = 28$  nm, the thickness of the diffusing layer containing 20% dPS tracer. Hence, most of the tracer chains in the diffusing layer are oriented. For lower values of  $\delta$ , the diffusion volume contains both oriented and nonoriented chains. From the data, with maximum  $\delta = 0.015$ , we obtain the diffusion coefficient of the fully oriented tracer layer to be  $D^* = 6.07 \times 10^{-16}$  cm<sup>2</sup>/s. The second regime corresponds to  $\delta = 0$  or a diffusion volume that is completely nonoriented. Hence, the diffusion coefficient is simply  $D_{\text{bulk}} = 11.7 \times 10^{-16}$  cm<sup>2</sup>/s. Therefore, for a given value of  $\delta$ , we can define the oriented fraction,  $\phi^{\text{oriented}} = L/L_0$ , where  $L$  is the penetration depth for a given number of rubbing cycles (Figure 1). The diffusion coefficient,  $D_{\text{surf}}$ , can be expressed by a combination of  $D^*$  and  $D_{\text{bulk}}$

$$D_{\text{surf}} = D^* \phi^{\text{oriented}} + D_{\text{bulk}}(1 - \phi^{\text{oriented}}) \quad (3)$$

In Figure 3b, we plot the measured  $D_{\text{bulk}}/D_{\text{surf}}$  as a function of  $\phi^{\text{oriented}}$ . The solid line is the value calculated from eq 3. From the figure, we see that reasonably good agreement is obtained without any free parameters.

**Surface Relaxation on a Rubbed Surface.** Tracer diffusion provides information on the long-range center-of-mass chain mobility. No information is obtained regarding the surface relaxation process. It is therefore interesting to probe the surface relaxation on the same sample as that on which long-range diffusion perpendicular to the plane was measured.

We have developed a SMFM technique that measures the local change in the surface modulus with temperature in an area less than 10 nm. The change in modulus is correlated to the creep and flow response of the film under deformation. The details of the method are described in ref 13. In brief, an AFM tip is placed in contact with the surface, and a sinusoidal modulation with an amplitude of 2 nm is applied parallel to the surface. The response signal of the cantilever,  $\Delta X$ , which is proportional to the area of contact between the tip and the sample surface<sup>13</sup> is detected with a lock-in amplifier. The amplitude of the response signal vs temperature for the rubbed and nonrubbed surface is plotted in Figure 4. The lower curve corresponds to an unrubbed ( $\delta = 0$ ) sample. In this case, the discontinuity occurs exactly at  $T = T_g$ , where the elastic modulus decreases by several orders of magnitude. On the rubbed sample, two discontinuities are observed. The first occurring at  $T = 347$  K indicates that the surface modulus decreases before the bulk  $T_g$ . This temperature is similar to that reported in ref 8, where the induced birefringence starts to decrease rapidly with temperature. The second change corresponds to a further decrease in the modulus at the bulk glass transition temperature.

In Figure 5, we plot the onset temperature of the first transition,  $T_k$ , as a function of  $\delta$ . From the figure, we can see that the first transition temperature is around 350 K for all films with  $\delta > 0.005$ . This is consistent with the assumption that the top layer reaches maxi-

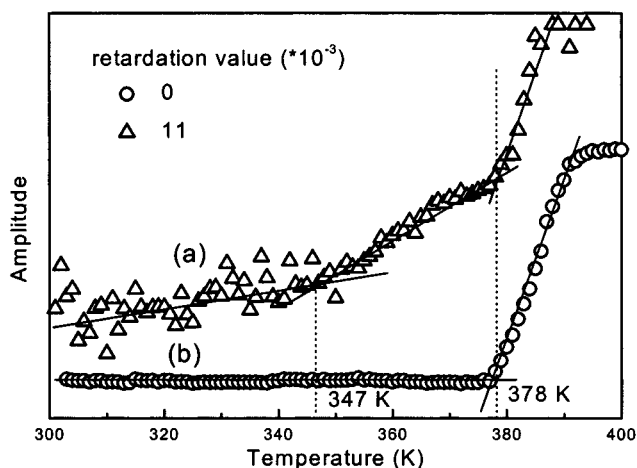


**Figure 4.** Amplitude of the response signal,  $\Delta X$ , as a function of temperature at the surface of a multilayer PS samples: (a) rubbed with  $\delta = 11 \times 10^{-3}$  and (b) nonrubbed.

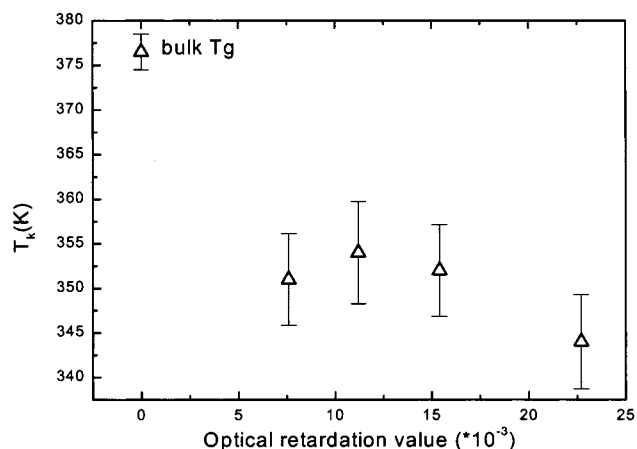


**Figure 5.** First surface transition temperature  $T_k$  vs optical retardation values for the multilayer samples.

um orientation immediately, after the first few rubbing cycles. The SMFM technique is sensitive to the relative modulus change of the very top layer but cannot determine the thickness of the modified layer. Hence, similar  $T_k$  values are seen for all of the films regardless of the extent of the oriented layer, as measured by  $\delta$ .

The surface relaxation can also be measured by observing the change in surface morphology of the rubbed film as a function of annealing temperature. Figure 6 shows a set of topographical scans of the surface of a rubbed sample with  $\delta = 0.015$ . As previously reported,<sup>16,17</sup> the rubbing process produces surface scratches and grooves as shown in Figure 6a. From the figure, we can see that the mean height of the scratches is less than 3 nm. The sample was annealed in situ on the AFM heating stage at given temperature for 10 min and then cooled to room temperature for imaging. From Figure 6a–d, we can see that the scratches and grooves start to become flatter even at temperatures lower than bulk  $T_g$ . In Figure 7, we plot the surface roughness (rms) as a function of annealing temperature. From the figure, we see that the scratches relax rapidly with temperature. The onset temperature  $T \approx 340$  K  $< T_g$  is similar to the temperature when the surface modulus was observed to decrease. This relaxation below  $T_g$  was also observed on molded surfaces where a square grating was inscribed<sup>18</sup> and in oriented liquid crystalline polymer glasses.<sup>19</sup> In ref 18, the relaxation rate for  $T < T_g$

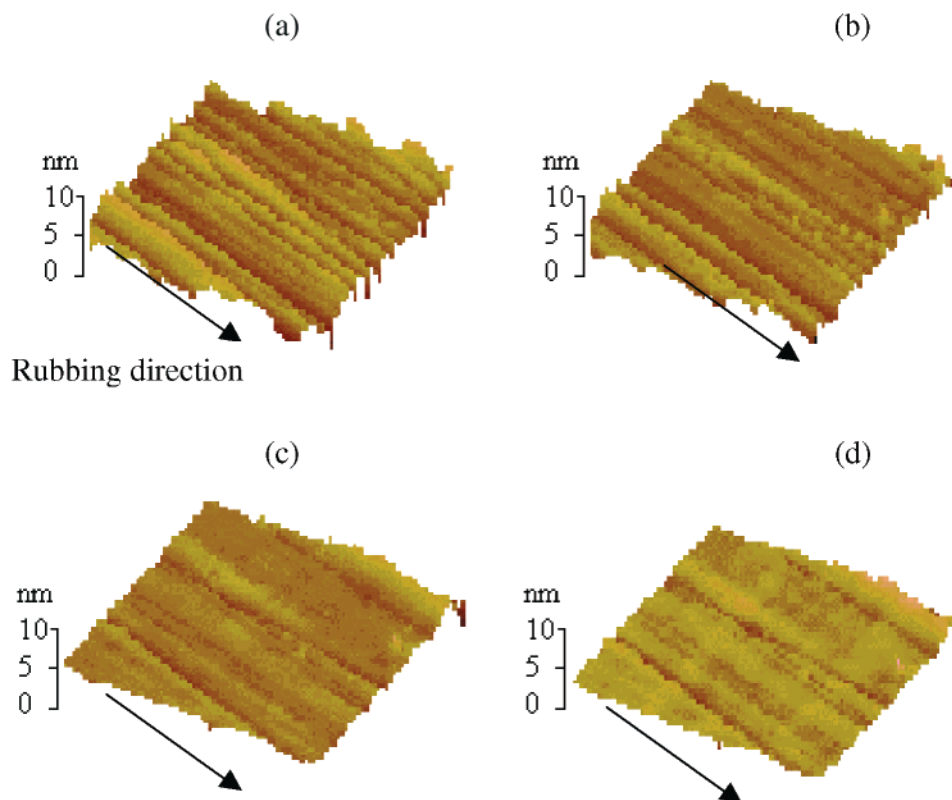


**Figure 6.** AFM topographical images of a rubbed multilayer sample annealed in situ on the AFM heating stage for 10 min at each of the following temperatures: (a) as-rubbed, (b) 360 K, (c) 380 K, and (d) 400 K. The scan size is  $6\ \mu\text{m} \times 6\ \mu\text{m}$  and the  $z$  range is 10 nm.

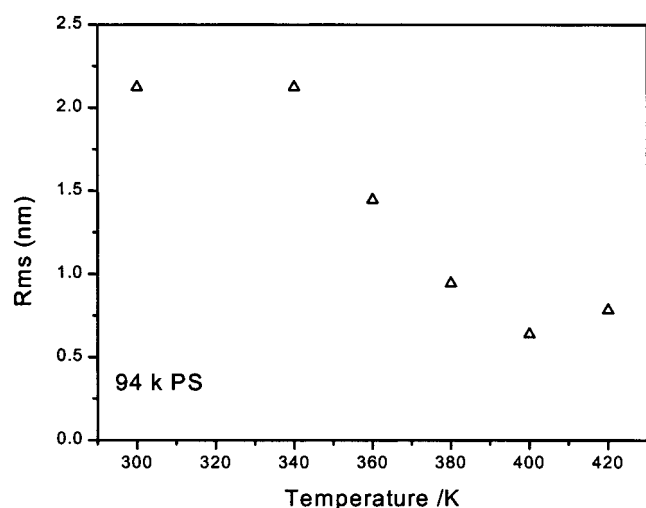


**Figure 7.** Rms roughness as a function of annealing temperature for the sample described in Figure 6.

was independent of the molecular weight of the polymer, which indicates that it was driven by elastic relaxation rather than viscous flow. The length scale of the relaxation, on the order of the rms roughness, or around 2 nm is comparable to the one detected by the SMFM method. Hence, the scratches and grooves can flatten via short-range motion of the chain without large center-of-mass diffusion.

These results show conclusively that surface relaxation occurs very quickly at  $T < T_g$ , in agreement with the optical birefringence measurement. On the other hand, the fact that we still observe a significant orientation effect on the diffusion normal to the rubbed surface indicates that the long-range center-of-mass motion is

much slower. In this study, a significant orientation effect on diffusion is observed at 407 K for several hours. At this temperature, all birefringence or surface roughness was already reduced to zero.

## Conclusion

In conclusion, we have measured the tracer diffusion coefficient in PS film oriented by surface rubbing. The result shows that the diffusion perpendicular to the rubbed surface is slower in oriented than nonoriented chains. On the other hand, surface relaxation related with stress is observed to occur at  $T \approx 340$  K, which is about 30 K lower than the  $T_g$  of PS.

**Acknowledgment.** Support from the NSF (DMR-0080604) is gratefully acknowledged.

## References and Notes

- (1) Zheng, X.; Rafailovich, M. H.; Sokolov, J.; Strzhemechny, Y.; Schwarz, S. A.; Sauer, B. B.; Rubinstein, M. *Phys. Rev. Lett.* **1997**, *79*, 241.
- (2) Frank, B.; Gast, A. P.; Russell, T. P.; Brown, H. R.; Hawker, C. *Macromolecules* **1996**, *29*, 6531.
- (3) Lin, E. K.; Wu, W.-L.; Satija, S. K. *Macromolecules* **1997**, *30*, 7224.
- (4) Forrest, J. A.; Dalnoki-Veress, K.; Stevens, J. R.; Dutcher, J. R. *Phys. Rev. Lett.* **1997**, *56*, 5705.
- (5) Keddie, J. L.; Jones, R. A. L.; Cory, R. A. *Europhys. Lett.* **1994**, *27*, 59.
- (6) Kajiyama, T.; Tanaka, K.; Takahara, A. *Macromolecules* **1997**, *30*, 289; *Polymer* **1998**, *39*, 4665.
- (7) Liu, Y.; Russell, T. P.; Samant, M. G.; Stohr, J.; Brown, H. R.; Cossy-Favre, A.; Diaz, J. *Macromolecules* **1997**, *30*, 7768.
- (8) Schwab, A. D.; Agra, D. M. G.; Kim, J.; Kumar, S.; Dhinjwala, A. *Macromolecules* **2000**, *33*, 4903.
- (9) Toney, M. F.; Russell, T. P.; Logan, J. A.; Kikuchi, H.; Sands, J. M.; Kumar, S. K. *Nature (London)* **1995**, *374*, 709.

- (10) Samant, M. G.; Stohr, J.; Brown, H. R.; Russell, T. P.; Sands, J. M.; Kumar, S. K. *Macromolecules* **1996**, *29*, 8334.
- (11) Van Aerle, N. A. J. M.; Barmantlo, M.; Hollering, R. W. J. *J. Appl. Phys.* **1993**, *74*, 3111.
- (12) Wei, X.; Zhuang, X.; Hong, S.-C.; Goto, T.; Shen, Y. R. *Phys. Rev. Lett.* **1999**, *82*, 4256.
- (13) Ge, S.; Pu, Y.; Zhang, W.; Rafailovich, M.; Sokolov, J.; Buenviaje, C.; Buckmaster, R.; Overney, R. M. *Phys. Rev. Lett.* **2000**, *85*, 2340.
- (14) Geary, J. M.; Goodby, J. W.; Kmetz, A. R.; Patel, J. S. *J. Appl. Phys.* **1987**, *62*, 4100.
- (15) Green, P. F.; Kramer, E. J. *J. Mater. Res.* **1986**, *1*, 202.
- (16) Pidduck, A. J.; Bryan-Brown, G. P.; Haslam, S.; Bannister, R.; Kitely, I.; McMaster, T. J.; Boogaard, L. *J. Vac. Sci. Technol.* **1996**, *A14*, 1723.
- (17) Kim, J.; Rosenblatt, C. *Appl. Phys. Lett.* **1998**, *72*, 1917.
- (18) Sharma, S.; Pu, Y.; Rafailovich, M.; Sokolov, J. APS VC12.02, Atlanta, 1999.
- (19) Chen, D.; Zachmann, *Polymer* **1991**, *32*, 1612.

MA002039U